

RELATION BETWEEN FIBRE FLEXIBILITY AND CROSS-SECTIONAL PROPERTIES

Marius Rusu,^{a,*} Kathrin Mörseburg,^b Øyvind Gregersen,^a Asuka Yamakawa,^a and Sari Liukkonen^c

The correlation between the fibre flexibility and cross-sectional area moment of inertia of thermomechanical pulp fibres was investigated. The main effects of refining were found to be internal fibrillation, external fibrillation, and fibre shortening. Internal fibrillation increases fibre flexibility and fibre collapsibility, improving fibre-to-fibre contact in a paper sheet. The raw materials used were pulps produced from six different Norway spruce logs and six different Scots pine logs, chosen in a manner that allowed variation of fibre wall thickness and fibril angle independently. Each wood sample was refined in four stages using a pressurized 12" Sprout Waldron single disc refiner. Fibre flexibility was assessed by FiberMaster bendability measurements. Fibre bendability was measured on the +48 Bauer McNett fractions of the twelve 2nd, 3rd, and 4th stage thermomechanical pulps (TMP). The fibre cross-sectional samples were imaged using scanning electron microscopy (SEM). An image analysis method to calculate the area moment of inertia of each fibre using numerical integration was developed. Fiber bendability increased with specific energy consumption for both wood species (spruce and pine) from the 2nd refining stage to the fourth refining stage. Spruce had a higher rate of bendability increase than pine upon refining. It was expected that fibres with a low area moment of inertia would result in higher bendability, but no such correlation was found for either spruce or pine. Fibre bendability increased with internal fibrillation, as assessed from Simons staining. These results imply that local damage of the fibre wall such as delaminations, kinks, and compressions was the main effect in increasing the flexibility through refining of TMP.

Keywords: Fibre bendability; Area moment of inertia; Mechanical pulp; Internal fibrillation; Fibre cross-sectional properties; Image analysis

Contact information: a: Norwegian University of Science and Technology, Høgskoleringen 6B, N-7491, Trondheim, Norway; b: Paper and Fibre Research Institute, Høgskoleringen 6B, N-7491, Trondheim, Norway; c: VTT Technical Research Centre of Finland, P.O. Box 1000, FI-02044 VTT, Espoo, Finland; *Corresponding author: marius.rusu@chemeng.ntnu.no

INTRODUCTION

Fibre Flexibility Measurement

Fibre flexibility is a pulp property that plays an important role in the manufacture of paper. Wet fibre flexibility influences paper properties such as apparent sheet density and porosity (Paavilainen 1993), paper strength properties (Forgacs 1963), surface smoothness, and optical properties (Paavilainen 1993).

Different methods to evaluate fibre flexibility have been developed. Some of these methods are single fibre based, while others evaluate the fibre network. Robertson has investigated the flexibility of fibres in a viscometer (Robertson et al. 1961). Fibres were suspended in a liquid and subjected to laminar shear fields. The fibres exhibited rotational orbits, which reflected individual flexibility. By looking at the fibres through a microscope, the bending of them could be studied. Another method for determining stiffness of fibres was developed by Samuelsson (1963). The fibre was fixed in a clamp as a cantilever to the wall of a channel with a laminar water flow. The bending of the fibre due to water stream was observed through a microscope. A similar method to measure fibre flexibility for individual fibres was used by Tam Doo and Kerekes (1981). The fibre was placed in a capillary tube and then immersed in a water bath. The fibre was observed through a microscope, and its maximum deflection is measured in a micrometer eye piece.

A fibre flexibility measurement method based on evaluating the fibre network was developed by Steadman and Luner (1985). In the Steadman method, fibres are wetted and pressed onto a thin support wire that was fixed on a glass slide. The fibre and the support wire are approximately 90° to one another so that when pressed onto the wire, the fibre forms an arch-like span over the wire as it deforms. The fibre is then allowed to dry, and the sections of the fibre in contact with the slide become adhered to the glass slide. The length of the section of span that is not in contact with the glass slide is measured from above, using a conventional light microscope. The free span length measurement is then used in the calculation of flexibility.

Petit-Conil (1994) measured fibre flexibility using Bauer-McNett classification and the average lengths obtained with a Kajaani FS100 apparatus. A static flexibility coefficient was defined using the correlation between the Kajaani lengths and the theoretical McNett lengths.

Kuhn (1995) developed a method that does not depend on single fibre manipulation. The fibres were placed in a capillary penetrating a main channel with water flowing through the capillary into the main channel flow. As the fibres exit the capillary tubes they are deflected and deformed, and their flexibility can be calculated using simple beam theory.

Yan and Li (2008) developed a method to measure the flexibility of individual wet fibres using confocal laser scanning microscopy (CLSM) and image processing on the basis of Steadman and Luner method. With CSLM, the freespan length and the deflection height can be directly determined from the fibre transverse view of the fibre span. The collapsibility and moment of inertia can also be measured from the fibre cross section obtained from CSLM. Thus, it was possible to measure the elastic modulus of individual fibres.

Fibre flexibility can also be assessed using a STFI FiberMaster analyser (Karlsson 1999), where the change in average fibre shape, as the fibres are subjected to different shear fields, is detected and denoted as bendability.

As mechanical pulp fibres are relatively stiff, short, and partly damaged, reliable flexibility measurements on individual fibres are difficult, and mechanical pulp fibre flexibility has thus rarely been assessed and documented.

Flexibility and Area Moment of Inertia

For homogenous materials the flexibility (F) is related to bending stiffness (S), area moment of inertia (I), and modulus of elasticity (E) through equation 1:

$$\frac{1}{F} = S = E \times I \quad (1)$$

For regular surfaces, like hollow tubes, an analytical solution to calculate the moment of inertia can be found. Equation 2 gives an example for a hollow tube.

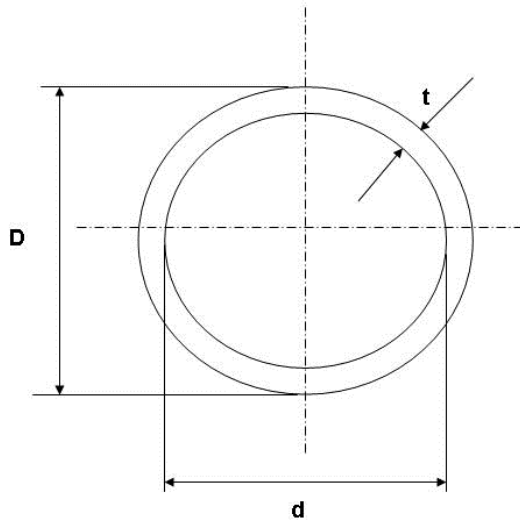


Fig.1. Thin – walled circular tube (Gere and Barry 2009)

$$I_p = \frac{\pi dt}{4} (d^2 + t^2) \quad (2)$$

In this equation I_p is the polar moment of inertia of the cross-sectional area of a tube, d is the average diameter, and t is the wall thickness.

The polar moment of inertia is analogous to the moment of inertia, which characterizes the ability of an object to resist bending. For irregular surfaces, such as fibres, a numerical solution instead of an analytical solution is used to calculate the area moment of inertia.

The following hypothesis is proposed:

A reduction in the area moment of inertia, which is a function of fibre wall thickness, is the main effect responsible for reducing fibre bending stiffness upon refining of a mechanical pulp.

The purpose of this study was to investigate the effect of area moment of inertia and internal fibrillation on the flexibility of TMP pulp fibres.

MATERIAL AND METHODS

Pulp Samples

Six different Norway spruce (*Picea abies*) logs and six different Scots pine (*Pinus sylvestris*) logs were selected and harvested in Finland. For the trials the wood logs were sawn to discs, which were debarked manually and chipped in a laboratory chipper, giving chips with even length and thickness (the width was cut manually with a knife). The logs were frozen before chipping and the chips were stored frozen before refining. The initial fibre lengths were measured from the delignified (laboratory kraft cooking) chips. The chipped samples were refined in four refining stages, by applying similar refining conditions for each raw material, using a pressurized 12" Sprout Waldron single disc refiner. In this study 36 mechanical pulps with different characteristics (high fibre wall thickness, low fibre wall thickness, high fibril angle and low fibril angle), were used. A brief description of the pulp samples is given in Table 1 (Rusu et al. 2009). The objective of this segregation was to independently evaluate the influence of wood species, tracheid wall thickness, and fibril angle on the development of some important TMP fibre properties. The average fibre wall thickness and fibril angle were measured using a SilviScan-device (Evans et al.1995) prior to refining.

Table. 1. Overview of Investigated Samples

Samples code	Symbol	Description
SwA	○	Spruce low fibre wall thickness low fibril angle
SwA	●	Spruce low fibre wall thickness, high fibril angle
SWa	○	Spruce high fibre wall thickness, low fibril angle
SWA	●	Spruce high fibre wall thickness, high fibril angle
SWa	○	Spruce high fibre wall thickness, low fibril angle
SWA	●	Spruce high fibre wall thickness, high fibril angle
Pwa	△	Pine low fibre wall thickness, low fibril angle
PwA	▲	Pine low fibre wall thickness, high fibril angle
PWa	△	Pine high fibre wall thickness, low fibril angle
PWA	▲	Pine high fibre wall thickness, high fibril angle
PWa	△	Pine high fibre wall thickness, low fibril angle
PWA	▲	Pine high fibre wall thickness, high fibril angle

Fibre Characterization

In this study mechanical pulp fibre flexibility was assessed through measurements of the fibre bendability with the commercial STFI FiberMaster instrument (Karlsson et al. 1999). This method was chosen because it is based on evaluating a large random selection of fibres and yields geometry-based bendability distributions.

The STFI FiberMaster provides distributions of fibre length, fibre width, and fibre shape (straightness) based on automatic and real time analysis of two-dimensional images of suspended pulp fibres. For bendability measurements the pump speed and resultant flow rate are increased by a factor of three in two additional measurement cycles.

The fibre bendability is calculated from changes in the mean fibre shape for fibre populations of different geometries (length and width-classes), introduced by hydrodynamic deflection through different suspension flow rates and resulting shear forces. This is a statistical measurement. Thus the bendability measurement does not resolve the bendability of individual fibres, but provides an average change of fibre shape for all individuals in a given geometric class. While forces act in a defined manner when e.g. the stiffness of a paper beam is determined, fibres are not aligned and/or fixed in a controlled manner respective to the acting forces upon the FiberMaster shape and bendability measurement. The FiberMaster shape factor refers to the relation between the fibre's largest extension and its length L , and represents a measurement of fibre deformation in the xy -plane. The fibre's largest extension is equal to the diameter D_s in the smallest circumscribed circle of the fibre, as illustrated in Fig. 2.

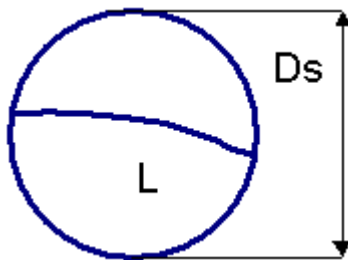


Fig. 2. Principle of fibre shape factor definition

The fibre shape factor ranges from about 50% to 100%, where 100% equals a completely straight fibre. The bendability range is about 0 to 15%, with lower values corresponding to less flexible fibres (Karlsson et al. 1999). If the mean fibre shape factor in a given population would decrease from 90% to 85% due to increased shear forces upon measurement, the mean bendability B_3 would be 5%.

The FiberMaster bendability is dependent on fibre length, cross-sectional geometry, and fibre wall structure (E-modulus) as well as technical measurement conditions (i.e. flow rates, temperature). Results were thus documented as discrete distributions for bendability in different geometric classes (length, width). The McNett fraction +48 was analysed for pulps taken after the 2nd, 3rd, and 4th stage refiner of each raw material. Five parallel measurements were conducted per sample with each sample containing approximately 5000 to 10000 fibres. Images were recorded using a camera with a resolution of 20 μm . As the mechanical properties of the fibres are temperature-dependent, bendability was determined in the temperature range 38 to 45 °C. The results were documented as mean bendability B_3 for the optical length class 1.5 to 3.0 mm, accounting for about 40 to 50% of all fibre material in the +48 fraction of the samples.

Loosening of the fibre wall structure, i.e. internal fibrillation, was examined using Simons' staining (Simons 1950; Yu 1995). Simons' stain is a two-colour differential stain that is sensitive to variations in the accessibility of the interior structure of fibres. When treated with a mixed solution of orange and blue dyes, fibres with internal fibrillation will stain blue, and fibres without internal fibrillation will stain orange in locations where internal delamination, fibrillation, or fibre damage has occurred. The McNett fraction for the Simons staining was +28 (combined R14 and R28). The dyes used were: Pontamine Sky Blue 6BX and Pontamine Fast Orange 6RN. The solutions were mixed in a ratio 1:1. Minimum 600 fibres per sample from at least four preparates were analysed. The general sample handling and staining were done based on standards SCAN-G 3 and 4.

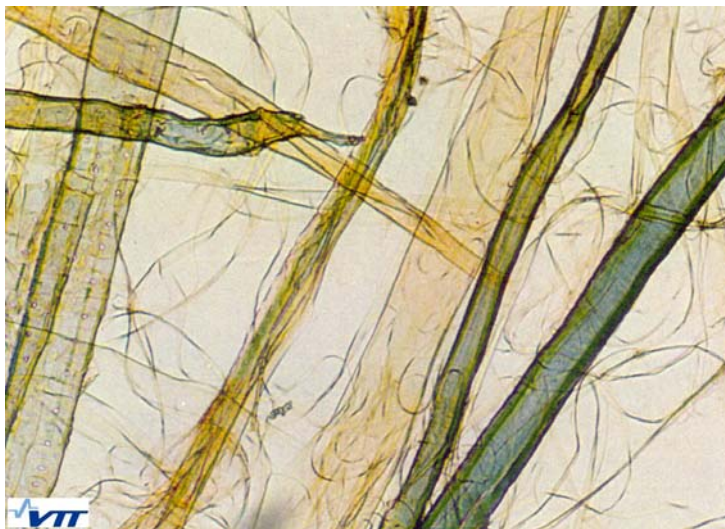


Fig. 3. Light microscope image of Simons' stained mechanical pulp fibres

Cross-sectional fibre characteristics were assessed for the +48 Bauer-McNett fractions of the pulps from 1st, 2nd, 3rd, and 4th refining stages for all twelve raw materials. Approximately 1000 fibres per sample were evaluated. The fibres were aligned in parallel, freeze dried, embedded in epoxy, ground, polished, and carbon coated (Reme 2001). Digital images were recorded in a Hitachi S-3000 VPSEM in BEI mode, 150 x magnification, giving a resolution of 0.3 $\mu\text{m}/\text{pixel}$. The images were binarized, filtered, and edited manually. Finally, the area moment of inertia and some other parameters were calculated for both intact and split fibres.

A new routine was developed to measure area moment of inertia. Area moment of inertia, in x and y direction is defined as,

$$I_x = \sum (y^2 A + I_{local}) \quad (3)$$

$$I_y = \sum (x^2 A + I_{local}) \quad (4)$$

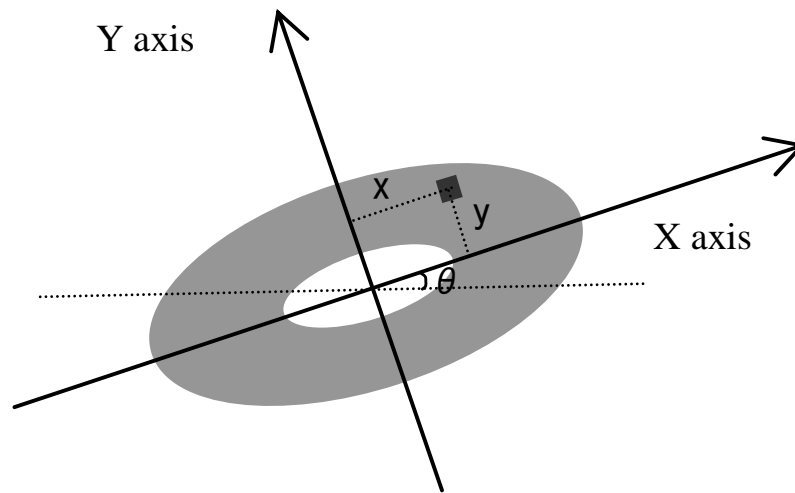


Fig. 4. Fibre cross-section, principal axis

where A is the surface area of one pixel, I_{local} is the second moment of inertia for one pixel of the composite in the appropriate direction, y is the distance between a pixel of interest and its orthogonal projection onto the X axis, and x is the distance between a pixel of interest and its orthogonal projection onto the Y axis pixel.

The X axis represents the lengthways direction of the object and bending around the X-axis and describes the weakest direction of an elliptic cross-section. The Y axis is perpendicular to the X axis, passes through the center of the object, and represents the direction of the highest bending stiffness.

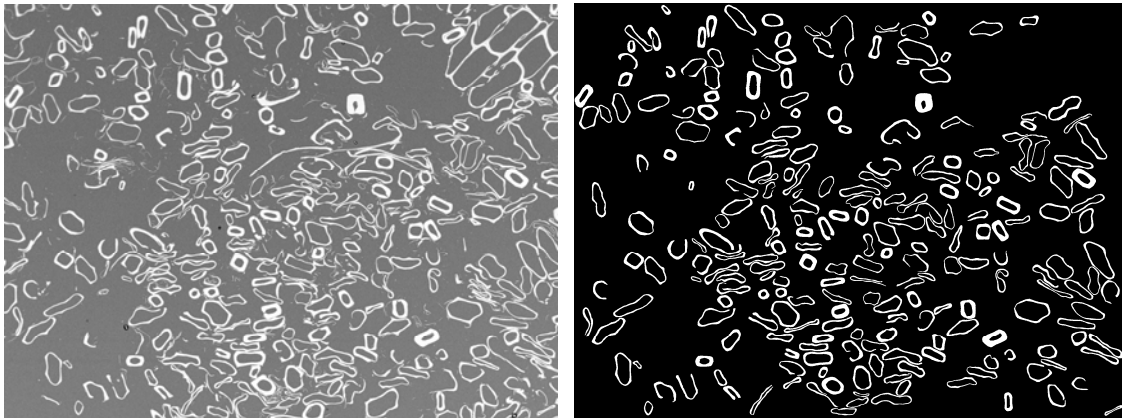






Fig. 5. SEM-BEI fibre cross-sectional images (left) and after binarisation and manual editing (right)

Table 2. Fibre cross-sections, together with their corresponding I_y and I_x values

Fibre	$I_y, \mu\text{m}^4$	$I_x, \mu\text{m}^4$
	21000	13000
	13000	1400
	10000	1800
	25000	8000

RESULTS AND DISCUSSION

Effect of Refining on Fibre Flexibility

Figures 6 and 7 show the relation between specific energy consumption and fibre bendability for Norway spruce and Scots pine. The results show that fibre bendability increases with specific energy consumption (SEC). This is in agreement with previous findings of Tchepel et al. (2006) and Hill et al. (2010) and with industry knowledge. For a given wood class, as defined by mean tracheid wall thickness and mean fibril angle, spruce TMP fibres had higher bendability than pine. Spruce had on average an increase in bendability of 1.70 units from 2nd to the 3th refining stage, and pine showed an increase of 0.60 units.

No significant trends in the initial level of bendability or development in bendability as a function of fibre wall thickness or fibril angle were seen. The error bars in Figs. 6 and 7 represent the mean standard deviation for the measured bendability.

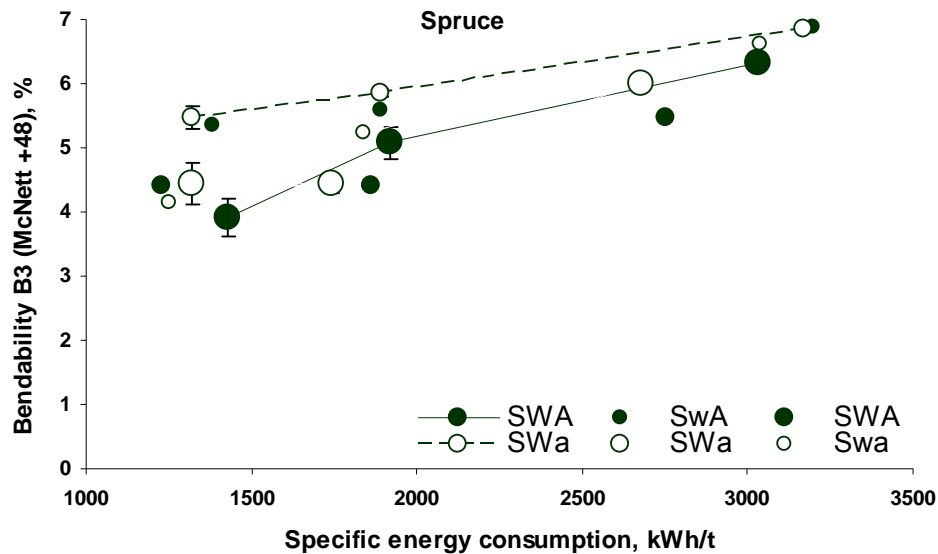


Fig. 6. Mean fibre bendability versus specific energy consumption (Norway spruce)

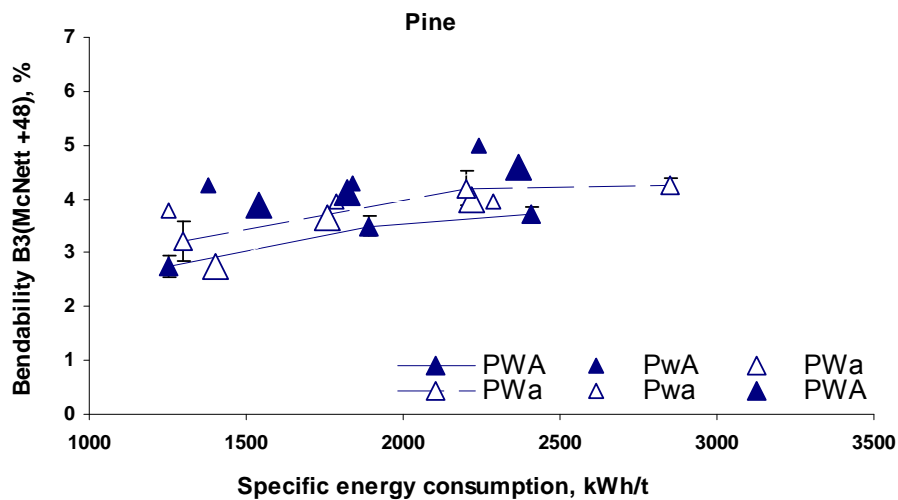


Fig. 7. Mean fibre bendability versus specific energy consumption (Scots pine)

Figures 8 and 9 show that bendability was not higher for fibres having a low moment of inertia. This is not in agreement with the previous findings of Tchepel et al. (2006). Tchepel calculated the flexibility of wood-pulp fibres using the elastic modulus E and the second moment of area I . The measurements for the topology of single fibres were done using a confocal laser scanning microscope, and the elastic modulus of the fibres was measured with single-fibre fatigue cell.

Thus no effect of the cross-sectional geometry on the measured bendability was found. This indicates that local damage of the fibre wall such as delamination, kinks, and compressions, was the main effect in increasing bendability with refining; this is in

agreement with previous findings (Kibblewhite 1972). Kibblewhite used microscopy to assess the effect of beating on fibre flexibility.

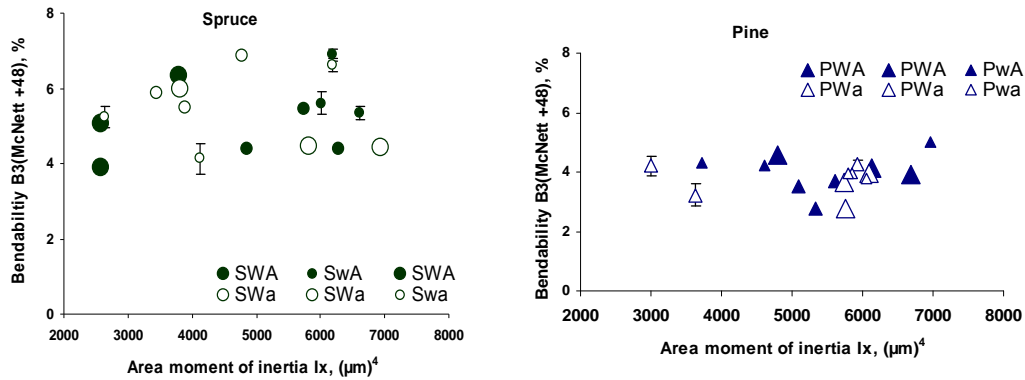


Fig. 8. Area moment of inertia in the weak direction (I_x) plotted against fibre bendability (spruce left, pine right)

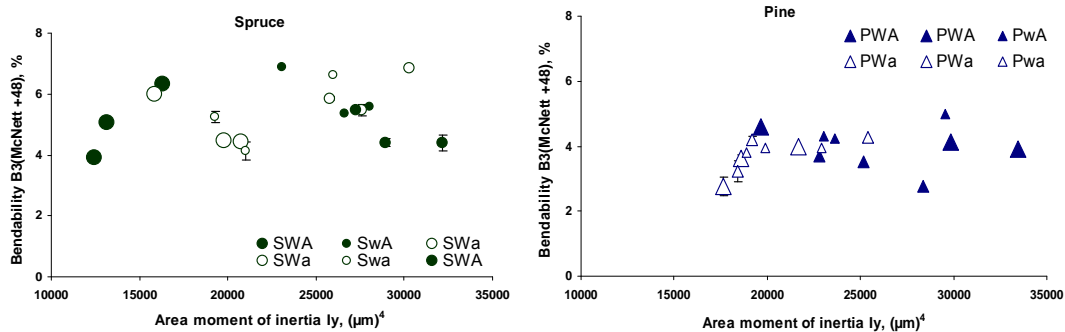


Fig. 9. Area moment of inertia in the stiffest direction (I_y) plotted against fibre bendability (spruce left, pine right)

No significant changes in area moment of inertia were seen as a function of specific energy consumption for any of the raw materials. This is not in agreement with the previous findings of Tchepele et al. (2006).

Figure 10 shows the mean fibre wall thickness of the pulp fibres plotted against energy consumption. Fibre wall thickness decreased with increasing energy consumption for both wood species. This is in agreement with previous findings (Reme and Helle 2001; Kure et al. 1999).

Distributions for the area moments of inertia were constructed for all samples. Figure 11 shows the distributions, in the stiffest direction (I_y) and in the weak direction (I_x), for a spruce pulp with thick walls and low fibril angle. It can be seen that the shape of the area moment of inertia curves did not change significantly during refining.

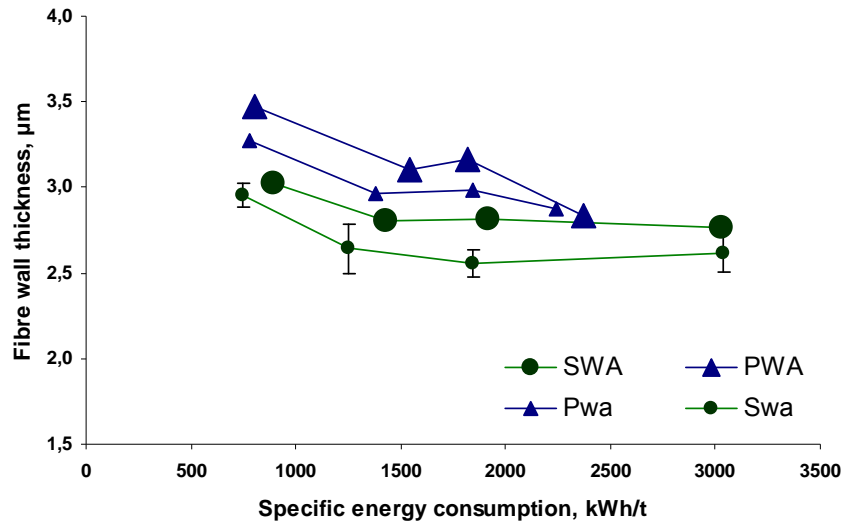


Fig. 10. Mean fibre wall thickness versus against specific energy consumption. Error bars represent the mean standard deviation for cell wall thickness

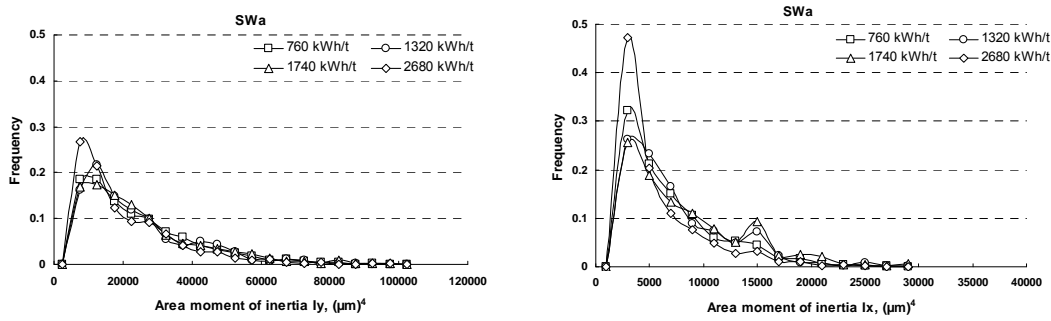


Fig. 11. Area moment of inertia distributions. Left: spruce pulps in the stiffest direction; Right: spruce pulps in the weak direction

Table 3. The Mean and Median Values for the Distribution Measured

Sample	kWh/t	$I_x, \mu\text{m}^4$		$I_y, \mu\text{m}^4$	
		Mean	Median	Mean	Median
SWA	760	19440	14766	5280	3675
	1320	19774	14094	5821	4069
	1740	20770	15354	6950	4822
	2680	15879	10622	3815	2224

Internal Fibrillation

Internal fibrillation reduces the bending stiffness of the fibre wall by reducing the effective *E* modulus, thus increasing wet fibre flexibility and collapsibility (Lammi and Heikkurinen 1997). Higher flexibility results in increasing interfibre bonding (Paavilainen 1994) and an increase in the strength properties (Kotik 2007). The results showed that fibre bendability increased with internal fibrillation for both spruce and pine

TMP samples (Fig. 12). In Fig. 13 internal fibrillation is plotted against specific energy consumption. We can see that internal fibrillation was increased with SEC, for both raw materials, and that the increase was slightly higher for spruce than pine. Spruce had on average 3% more increase in internal fibrillation than pine. This confirms that internal fibrillation is the most important factor affecting bendability.

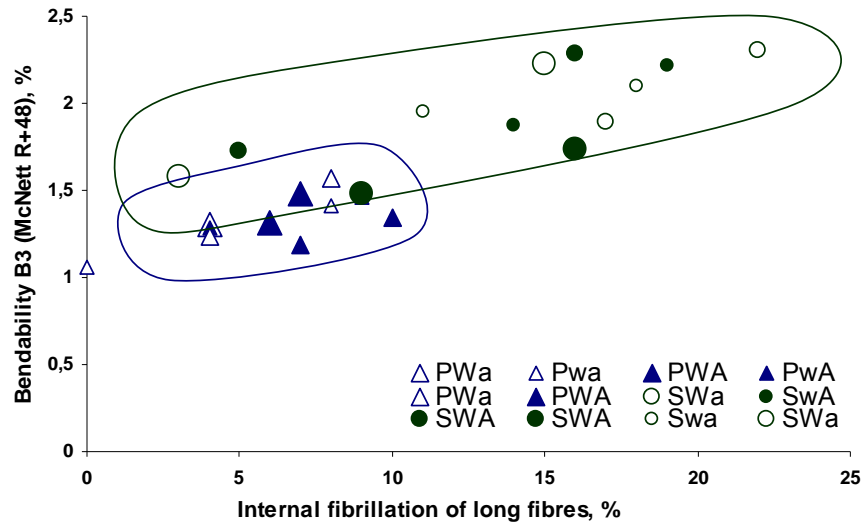


Fig. 12. Fibre bendability plotted against internal fibrillation of long fibres

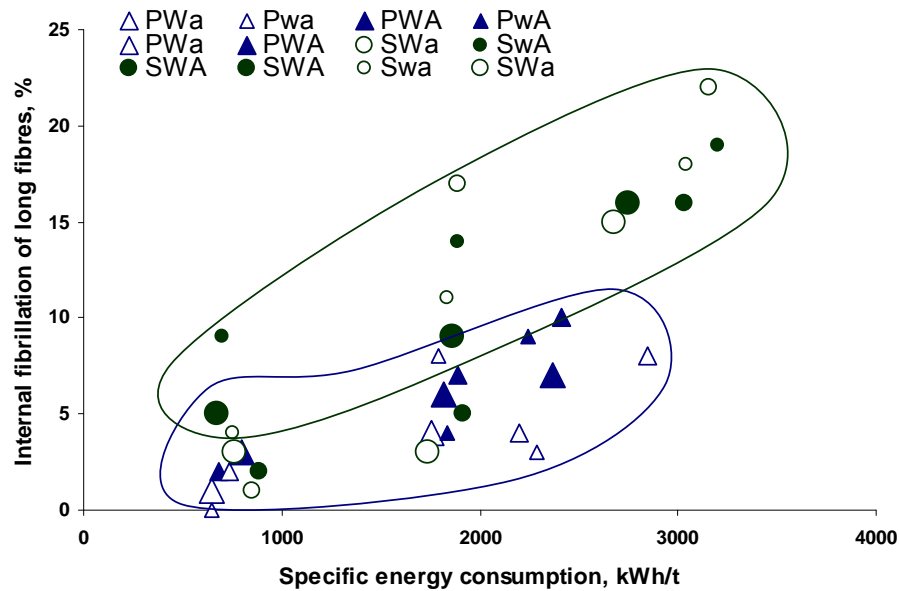


Fig.1 3. Internal fibrillation of long fibres (McNett +28) versus specific energy consumption

DISCUSSION

The Mechanism of Increasing TMP Fibre Bendability by Refining

For structures that have no internal damage, the bending stiffness is proportional to the area moment of inertia. But as Figs. 8 and 9 clearly show, this is not the case for TMP fibres. On the contrary, doubling of the area moment of inertia had no significant effect on the measured bendability. The internal fibrillation on the other hand increased linearly with measured bendability. It seems probable that such localised internal fibrillation has a much higher effect on the measured bendability than the original bending stiffness. Therefore, the bending stiffness of more undamaged fibre parts between the kinks and microcompressions does not have a significant effect on the measured bendability.

CONCLUSIONS

1. Based on the theory of Tchepel et al. (2006) a hypothesis was tested that fibres with low area moment of inertia would be more flexible. The results of bendability measurements do not support this hypothesis. The hypothesis that increasing flexibility during refining is caused by a reduction in the area moment of inertia is therefore not confirmed. This indicated that local damage of the fibre wall, such as delamination, kinks, and compressions, was the main effect in the increasing of the bendability with refining.
2. Fibre bendability increases with specific energy consumption upon mechanical pulp refining. For the investigated refining stages the most significant increase in fibre bendability occurred from the 2nd to the 3rd stage. Spruce had on average an increase in bendability with 1.70 units from the 2nd to the 3th refining stage and pine with 0.60 units. Spruce TMP fibres were more flexible than pine fibres after refining.
3. The results showed that fibre bendability increases with internal fibrillation and that spruce has a higher increase in flexibility than pine. Internal fibrillation increases with SEC, for both raw materials, and is slightly higher for spruce than pine.

ACKNOWLEDGMENTS

The authors gratefully acknowledge the project funding from the Nordic Energy Research and the Stiftelsen PFI. We would also like to thank the PFI personnel for their help in this study.

REFERENCES CITED

- Evans R., Gartside G., and Downes, G. (1995). "Present and prospective use of Silviscan for wood microstructure analysis," *49th APPITA Annual General Conference*, Hobart, Tasmania, 91-96.

- Forgacs, O. L. (1963). "The characterization of mechanical pulps," *Pulp Paper Mag. Can.*, Convention Issue 64(C), 89-118.
- Hill, J., M. Sabourin, L., Johansson, K., Mörseburg, P., Axelsson, Aichinger, J., Braeuer, P., and Gorski, D. (2010). "Combining selective bleaching chemistries and ATMP technology for low energy mechanical pulping at higher brightness," 7th International Seminar on Fundamental Mechanical Pulp Research, Nanjing, China, June 21-23, 164-176.
- Karlsson, H., Fransson, P.-I., and Mohlin, U.-B. (1999). "STFI FiberMaster," 6th *Int. Conf. on New Available Technologies*, Stockholm, SPCI, 367-374.
- Gere, J. M., and Goodno, B. J. (2009). *Mechanics of Materials*, 7th edition, 230-231.
- Kibblewhite, R. P. (1972). "Effects of beating on fibre morphology and fibre surface structure," *Appita* 26(3), 196-202.
- Kotik, O. (2007). "Simulation of tensile properties of paper in the z-direction," *Nord. Pulp Paper Res. J.* 22(1), 28-34.
- Kuhn, D. C. S., Lu, X., Olson, J. A., and Robertson, A. G. (1995). "A dynamic wet fibre flexibility measurement device," *J. Pulp Paper Sci.* 21(10), 337-342.
- Kure, K.A., Dahlqvist, G., Sabourin, M. J. and Helle, T. (1999). "Development of spruce fibre properties by a combination of a pressurized compressive pretreatment and high intensity refining," *Proceedings TAPPI International Mechanical Pulping Conference*, Houston, TX, USA, 24-26 May, 427- 433.
- Lammi, T., and Heikkurinen, A. (1997). "Changes in fibre wall structure during defibration," *Fundamentals of Papermaking Materials Trans., 11th Fundamental Research Symposium*, Cambridge, UK, September, Vol.1, 641-662.
- Paavilainen, L. (1993). "Conformability – flexibility and collapsibility – of sulphate pulp fibre," *Paperi Puu* 5(9-10), 689-702.
- Paavilainen, L. (1994). "Bonding potential of softwood sulphate pulp fibres," *Paperi Puu* 6(3), 162-173.
- Petit-Conil, M., Cochaux, A. and Choudens, C. (1994). "Mechanical pulp characterization: a new and rapid method to evaluate fibre flexibility," *Paperi Puu* 76(10), 657-662.
- Reme, P. A. and Helle, T. (2001). "Quantitative assessment of mechanical fibre dimensions during defibration and fibre development," *J. Pulp Paper Sci.* 27(1), 1-7.
- Robertson, A. A., Meindersma, E., and Mason, S. G. (1961). "The measurement of fibre flexibility," *Pulp Paper Mag. Can.* 62 (1), 3-10.
- Rusu, M., Gregersen, Ø., Liukkonen, S., and Sirviö, J. (2009). "The influence of fibre wall thickness and fibril angle in fibre development in the TMP process," *Proceedings IMPC*, Sundsvall, Sweden, 91-95.
- Samuelsson, L. G. (1963). "Measurement of the stiffness of fibres," *Svensk Papperstidning* 66(15), 541-546.
- Simons, F. L. (1950). "A stain for use in the microscopy of beaten fibres," *Tappi* 33(7), 312-314.
- Steadman, R., and Luner, P. (1985). "The effect of wet fibre flexibility of sheet apparent density," *Papermaking Raw Materials Trans., 8th Fundamental Research Symposium*, Oxford, Vol. 1, 311-337.

- Tam Doo, P. A., and Kerekes, R. J. (1981). "A method to measure wet fiber flexibility," *Tappi* 64(3), 113-116.
- Tchepel, M., Provan, J. W., Nishida, A., and Biggs, C. (2006). "A procedure for measuring the flexibility of single wood-pulp fibres," *Mechanics of Composite Materials* 42(1), 83-92.
- Yan, D. and Li, K., (2008). "Measurement of wet fiber flexibility by confocal laser scanning microscopy," *J. Mater Sci.* 43, 2869-2878.
- Yu, X., Minor, J., and Atalla, R. (1995). "Mechanism of action of Simons' Stain," *Tappi J.* 78(6), 175-180.

Article submitted: October 12, 2010; Peer review completed: November 30, 2010;
Revised version received and accepted: January 6, 2011; Published: January 10, 2011.